Fabric as a Sensor: Towards Unobtrusive Sensing of Human Behavior with Triboelectric Textiles

Ali Kiaghadi
University of Massachusetts Amherst
College of Information and Computer Sciences, Amherst, MA, USA
akiaghadi@umass.edu

Morgan Baima
University of Massachusetts Amherst
Department of Chemistry
Amherst, MA, USA
mbaima@umass.edu

Jeremy Gummeson
University of Massachusetts Amherst
College of Information and Computer Sciences, Amherst, MA, USA
gummeson@cs.umass.edu

Trisha Andrew
University of Massachusetts Amherst
Department of Chemistry
Amherst, MA, USA
tandrew@umass.edu

Deepak Ganesan
University of Massachusetts Amherst
College of Information and Computer Sciences, Amherst, MA, USA
dganesan@cs.umass.edu

ABSTRACT

Smart apparel with embedded sensors have the potential to revolutionize human behavior sensing by leveraging everyday clothing as the sensing substrate. However, existing textile-based sensing techniques rely on tight-fitting garments to obtain sufficient signal to noise, making it uncomfortable to wear and limiting the technology to niche applications like athletic performance monitoring.

Our solution leverages functionalized fabric to measure the triboelectric charges induced by folding and compression of the textile itself, making it a more natural fit for everyday clothing. However, the large sensing surface of a functionalized textile also increases body-coupled noise and motion artifacts, and introduces new challenges in how we suppress noise to detect the weak triboelectric signal. We address these challenges using a combination of textile, electronics, and signal analysis-based innovations, and robustly sense joint motions by improving SNR and extracting highly discriminative features from the signal. Additionally, we demonstrate how the same sensor can be used to measure relative changes in skin moisture levels induced by sweating. Our design uses a simple-to-manufacture layered architecture that can be incorporated into any conventional, loosely worn textile. We show that the sensor has high performance in natural conditions by benchmarking the accuracy of sensing several kinematic metrics as well as sweat level. Additionally, we provide real-world performance evaluations across three application case studies including activity classification, perspiration measurements during exercise, and comfort level detection for HVAC systems.

SenSys '18, November 4–7, 2018, Shenzhen, China

ACM ISBN 978-1-4503-5952-8/18/11…$15.00
https://doi.org/10.1145/3274783.3274845

CCS CONCEPTS

• **Applied computing** → **Health care information systems**; • **Human-centered computing** → *Ubiquitous and mobile computing systems and tools*;

KEYWORDS

Ubiquitous sensing, smart textile

ACM Reference Format:
Ali Kiaghadi, Morgan Baima, Jeremy Gummeson, Trisha Andrew, and Deepak Ganesan. 2018. Fabric as a Sensor: Towards Unobtrusive Sensing of Human Behavior with Triboelectric Textiles. In *The 16th ACM Conference on Embedded Networked Sensor Systems (SenSys '18), November 4–7, 2018, Shenzhen, China.* ACM, New York, NY, USA, 12 pages. https://doi.org/10.1145/3274783.3274845

1 INTRODUCTION

While much of the recent research in the wireless sensing community has surrounded wearable technology like wristbands, phones, and glasses, one area that has seen relatively little work is smart apparel i.e. the integration of wearables in clothing. But the market for smart garments has grown steadily and is projected to have one of the highest growth rates among wearables over the next few years [11]. There is also increasing commercial activity including projects like Google Jacquard [2], and smart apparel from major clothing manufacturers like Nike, Under Armour, Ralph Lauren, and Levi's [3–6].

From a sensing perspective, a major advantage of smart clothing is the ability to monitor the signal directly at the location where the signal is strongest. In the context of joint sensing, it allows us to measure at the joint and not be limited to locations such as the wrist or waist. The ability to measure individual joints can enable many applications. For example, the knee and ankle joints are important to monitor gait disorders that can occur due to neurological causes like Dementia and Parkinson's, as well as non-neurological causes such as Osteoarthritis, intoxication, and medications (e.g. sedatives). The ability to measure joint movements is also an essential part of balance, posture, and motor control rehabilitation from conditions like stroke, as well as for mass-market athletic performance monitoring.

But a key drawback of existing textile-based joint sensing technology is that these generally only work with tight-fitting garments,

i.e. when the textile is worn as a *second skin*. This is for two reasons: a) stretch sensing-based methods [21] use tight-fitting textiles to increase stretch during joint movement, and b) other modalities like IMU and EMG rely on tight-fitting garments to reduce noise by improving skin contact and reducing motion artifacts.

However, a second skin is uncomfortable to wear on a regular basis, and we need new designs that can be used with loose-fitting, everyday clothing. We argue that in-order to achieve this goal, we need a radical shift in how we think about smart clothing. Rather than integrate traditional sensors like an IMU or stretch with the textile, we need a clean-slate approach that leverages the unique properties of the textile to enable entirely new ways of sensing using clothing. Specifically, a textile folds, compresses, twists, and scrunches during movement of the joint, and if we can find a way to measure these changes, it can offer an alternate *fabric-based* way of measuring joints while not requiring tight-fitting clothing.

To enable such fabric-based sensing capability, we build on recent work in functionalized triboelectric textiles — triboelectric textiles comprise layers that transfer surface charge from one layer to another and generate a voltage or current upon separation [28, 35, 36]. The advantage of triboelectric textiles for our problem is two-fold: a) since charge transfer between triboelectric textile layers happens due to the relative movement of the layers, it should allow us to measure the changes in the textile during joint movement even when wearing loose-fitting garments, and b) since the textile itself is the sensor, it allows us to leave the joint free of discrete electronics and wires, and place signal conditioning and other electronics at more convenient locations away from the joint.

While a triboelectric textile presents an exciting opportunity, we understand very little about its practicality for sensing when integrated into everyday clothing. We are certain to encounter a host of noise issues including electromagnetic noise, static potentials, and motion artifacts. These noise issues are exacerbated due to the large surface offered by textiles and the loose fit, and introduce challenges in how we recover a weak triboelectric signal and sufficiently suppress noise.

We address these issues and present the design of a novel fabric-based triboelectric joint sensor, Tribexor, that is simple to manufacture and is able to accurately detect individual joint motions while integrated with loosely worn clothing. The sensor system involves a co-design of the textile and electronics that tackles noise removal and signal enhancement by a combination of textile domain and electronics domain approaches. The final design of Tribexor consists of several discrete, stacked fabric layers that are stitched together and connected to a small form factor, low power amplification circuit and an embedded radio. We then look in detail at the signal output of the Tribexor sensor and try to explain the signal behavior from first principles, and extract highly discriminating and explainable features that allow us to detect joint movement, separate joint extension versus flexion, and estimate joint velocity.

While our original intent was to leverage such textiles for joint sensing, we stumbled upon an interesting observation during our experiments. We noticed that our sensor can also be used to measure sweating behavior since the triboelectric textile itself undergoes changes due to exposure to sweat. This provides a sensor reading that is equivalent to an Electrodermal Activity (EDA) sensor (alternately referred to as Galvanic Skin Response or GSR [20]). The ability to monitor joint movements together with sweat levels opens up additional applications such as improving comfort by adjusting HVAC settings and monitoring hydration while exercising.

In summary, the main contributions of this work are:

- We present Tribexor, a novel fabric-based triboelectric joint sensing system that can be integrated with loose-fitting clothing and senses joint flexion and extension, joint velocity, and sweat level.
- We show that Tribexor has 95.1% accuracy for detecting flexion and extension for elbow and knee joints, 88.8% accuracy for estimating elbow angular velocity, and 83.0% accuracy when estimating knee angular velocity. Additionally, we demonstrate the ability to detect moisture at the joint induced by sweating.
- We present two case studies: 1) activity recognition where Tribexor distinguishes between typical arm-based activities with 91.3% accuracy, and 2) thermal comfort detection that demonstrates Tribexor can be used to sense relative skin moisture levels that correspond to sweating.

2 RELATED WORK

The ultimate goal of this work is to develop a truly wearable joint sensor, i.e. one that is unobtrusive and integrated seamlessly into our everyday lives. Most existing sensor solutions fall short of this goal.

Discrete wearable sensors: Several prior efforts have used discrete sensors like IMUs and EMG electrodes for sensing joint movements. But this poses two challenges. The first challenge is that these sensors require tight contact to reduce motion artifacts due to the sensor moving around, so they do not work with loose clothing. The second challenge is that placing rigid sensor circuits at or close to the joint makes it prone to wear since the joint is in constant motion. Several efforts attempt to reconstruct joint movements by leveraging the signal from IMUs that are not placed at the joint itself, but at comfortable locations like the wrist [27]. However, this leads to a loss in accuracy — a wrist-worn IMU senses an aggregation of elbow, shoulder, and body movements which are hard to separate in an accurate manner.

Textile-based stretch sensors: In the textile domain, the most commonly used method for joint sensing is using conductive threads that change their resistance when stretched. But this approach is also reliant on tight wear to generate sufficient stretch upon movement. As a result, it is primarily used in athletic performance wear [1].

A notable exception is work by Gioberto and Dunne [14] which demonstrates a specialized overlock stitch pattern to induce stretch in the seam of denim jeans. The idea is clever but difficult to generalize to clothing that does not have such a thick seam at the joint.

Textile-based triboelectrics: There has been substantial interest in triboelectric generators (TEGs) in the material science research community [12, 15, 18]. TEGs convert small force inputs into an electrical (voltage and current) output. Because these devices operate by detecting surface potential changes created upon contact and release of dissimilar surfaces (due to either the triboelectric effect or contact electrification), micro- and nanostructured surfaces are needed to optimize voltage output. Such surfaces are typically generated on plastic or rigid glass substrates using various lithographic techniques.[31, 32, 34] Selected endeavors to create

Table 1: Challenges faced by wearable joint sensing technologies

Technology overview	Tightness	Accuracy	Robustness	Fabrication	References
Discrete wearable sensors	Wrist wearable	Low	High	Wearable electronics	[27]
Textile-based stretch sensing	Varies	Medium	Medium	Complex stitch pattern	[13, 14]
Textile-based triboelectrics	Stretch fit	Unknown	High	Self contained nano-fibers	[12, 28]
In-Situ perspiration sensing	Stretch fit	Medium	Medium	Textile sensing	[10]

fabric-like polymer composites are known but these approximations lack the inherent comfort, flexibility and breathability of natural textiles.[18, 25, 26]. From a sensing perspective, the focus of TEG research has primarily been on sensing tactile interaction with triboelectrics [17, 36] as opposed to body movements. In addition, work on triboelectric textiles has been in relatively clean lab environments free from all of the noise sources and motion artifacts introduced in actual wear [33]. Our work differs from this body of work in its focus on natural textiles, body movement sensing, and real-world environments,

In-situ Perspiration sensing: Tribexor not only measures joint motion but also a user's level of perspiration. Clinical gold-standard measures for perspiration sensing include weighing collected sweat generated or weighing an athlete before and after exercise [9]. But more recently there has been significant work on measuring various biochemical markers from sweat. These techniques generally use dedicated microchips or discrete humidity sensors that need to be placed at the sweating location (via integration with textile or wearable) [29]. Our work is unique in two ways: a) we use the fabric to simultaneously provide joint movement and perspiration information and b) we require no sensor electronics at the joint.

3 TEXTILE – ELECTRONICS CO-DESIGN

The overall hardware design of Tribexor consists of a smart textile sensor integrated with a small form factor electronic circuit used for amplification and signal conditioning. The sensor consists of a triboelectric-optimized textile patch and is used to collect electrical charge generated by the textile; a multi-stage amplifier circuit is used to amplify the voltage of the tribo signal and reject noise.

The central challenge that we address in the hardware design of Tribexor is how to get sufficiently strong signal to noise ratio (SNR) from the textile to detect states of interest. This overall challenge in turn can be broken down into two parts: a) the first step is to get sufficient transferred charge via triboelectricity such that the states are detectable, and b) the second step is to minimize noise from various sources to improve SNR. We look at these two challenges.

3.1 Maximizing triboelectric charge transfer

Overview of triboelectric textile sensing: Before we describe how we maximize transferred charge, we need to present some preliminaries regarding triboelectric textiles. Triboelectric textiles fundamentally measure motion via charge transfer. While there is still some debate over the mechanism of charge transfer in triboelectric devices [22], their operation in vertical contact mode is generally understood as depicted in Figure 1. When two dielectric layers come into contact, static charging occurs over the contacting surface area.

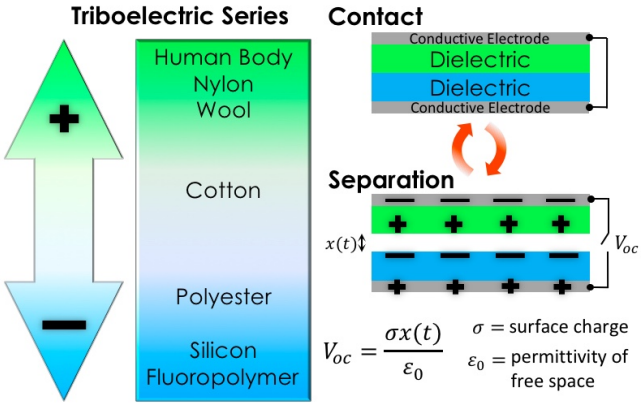

Figure 1: A triboelectric surface charge transfer mechanism induces a voltage on the textile electrodes when the textile and attached joint are bent.

Overall, the charge on the device remains at zero due to the charges being located in the same plane. Upon subsequent separation of the dielectric layers and therein the charges, an alternating current between the electrodes is induced to compensate for the charge imbalance; the generated charges are collected on conductive layers adjacent to the dielectric layers. Thus, open-circuit voltage is dependent on the surface charge density (σ), separation distance ($x(t)$) between dielectric layers, and permittivity of free space (ϵ_0).

Increasing triboelectric surface charge transfer: When optimizing a triboelectric textile for sensing, the critical parameter under our control is surface charge density (σ), since this defines the overall sensitivity of the magnitude of generated voltage to joint motion ($x(t)$). Our first goal is therefore to design the fabric to maximize surface charge transfer.

We start with cotton as our preferred textile material due to its widespread use. As shown in Figure 1, the surface charge density of pristine cotton is quite low, and is well below what is needed to sense movement. To increase charge transfer to higher levels that we can detect, the cotton lycra fabrics are functionalized in separate solutions [7] with different silane moieties, one containing an amine group that acts as the positively-charging triboelectric surface, and the other containing a fluorocarbon chain group that acts as the negatively-charging triboelectric surface. Sewn to the back of each functionalized layer is a set of electrode strips made of commercially-available conductive silver nylon fabric.

Our approach to functionalize fabric also makes it more suitable for loosely worn clothing. Since we can use a large functionalized

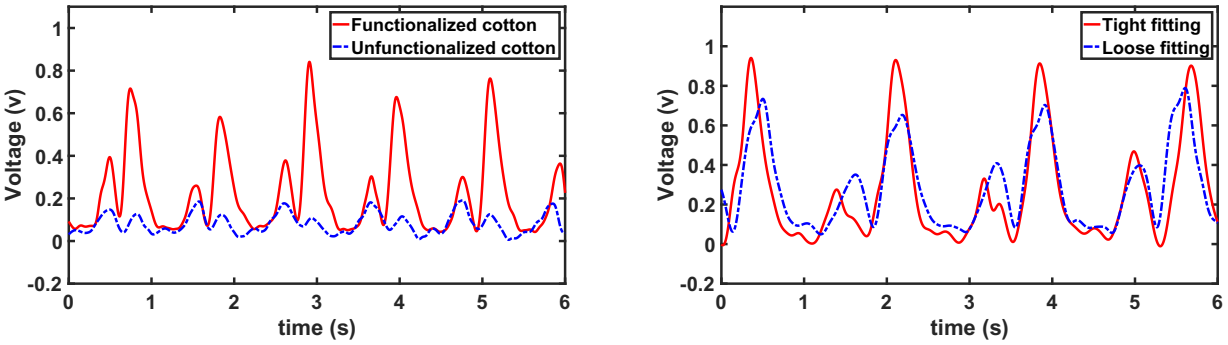

(a) pristine vs. functionalized signal output

(b) Loose vs. tight textile wear configurations

Figure 2: The voltage amplitude of sensed elbow joint motions is stable for a normal-sized, loosely worn elbow sleeve after functionalizing in solution.

triboelectric patch, we can cover most of the area that undergoes movement and aggregate the resulting charge. For example, in the case of the elbow joint, the functionalized fabric covers the entire front of the elbow.

Demonstrating the effect of functionalization: To demonstrate the advantage of our approach, we place a pristine textile sleeve over a user's elbow joint and ask them to perform several flexions and extensions in a clean electromagnetic environment. We measure the output voltage after amplification and show the measured voltage in Figure 2a in blue. We have the same user perform the same speed flexion and extension movements in the same environment, this time with a functionalized textile of the same geometry. We align the peaks corresponding to motion and plot the measured voltage in red (Figure 2a). We can see that the higher surface charge density of the functionalized textile results in an order of magnitude increase in signal amplitude.

Figure 2b demonstrates the effect of tightness of fit on the signal. We have a user wear Tribexor in two configurations: a) in loose configuration, the sensing textile is worn over a sweatshirt and an inner shirt i.e there are multiple layers of loose clothing under the sensor, and b) in tight configuration, a sleeve that is moderately tight fitting is worn directly over the skin. In both cases, the user repeats identical elbow motions. As shown in the figure, we find that the triboelectric voltage output is not very sensitive to tightness, demonstrating its potential for integration into everyday clothing.

The current textile design is a vertically integrated arrangement of fabric layers; while this design is simple to manufacture, we envision a more tightly integrated design that collapses layers into a thinner form factor. Our design shares elements similar to those found in nanoelectronics efforts that combine triboelectric primitives within a single thread [35].

3.2 Dealing with noise sources

The large surface area offered by a functionalized textile is a double-edged sword. On one hand, it aggregates the signal and increases SNR. On the other hand, it presents a large conductive surface which acts as a large antenna that absorbs more noise from the environment and the body.

Noise sources: There are two primary sources of noise that we need to deal with in Tribexor. The first is *electromagnetic noise*. Body coupled sensors with large surface area are significantly vulnerable to injection of low frequency interference injected by the nearby environment. In particular, 60 Hz noise is ubiquitous anywhere near powered infrastructure, resulting in coupling changes that occur because of the changes in effective surface area (folds and wrinkles) and tightness of contact with skin as the elbow joint opens and closes.

The second source of noise is *static field coupling*. Ideally, a triboelectric joint sensor will only measure the motion of the attached joint. But this is not always the case – in addition to electromagnetic noise sources, significant changes in body voltage potential can occur as a result of other body motions and triboelectric charge transfers between a user's body and the outside environment.

Why is it hard to reject EM and static field noise? While the sources of noise are similar to those observed for other modalities including ECG, EMG, and EOG, there are important differences. The first is form-factor. An electrode has a tiny footprint compared to a textile which acts as a much larger noise-absorbing antenna. In addition, when the tribo-textiles are used on loose clothing, the distance between the fabric and skin changes constantly due to body movements unlike electrodes that are attached to the skin. This results in continuous changes in the coupling capacitance, making it harder to predict and deal with the noise. The second is placement. Since electrodes are placed on the skin, different electrodes in contact with body absorb similar noise power in their electrodes. A differential amplifier can therefore reject this noise while letting the signal through (e.g. in the case of ECG, the electrical signal from the heart is stronger at one electrode and weaker at the other but the noise is similar). In our case, fabric layers are stacked vertically i.e. they have different separations from the skin. As a result, the inner electrode is affected by body coupling noises while the outer contact is absorbing noises from environment. This asymmetry means that

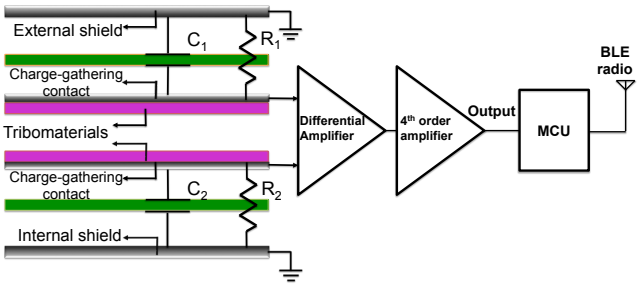

Figure 3: Here we show the design of Tribexor — the charge collection layers are fed to hardware filtering stages, digitized using a microcontroller's ADC and transmitted using a BLE radio

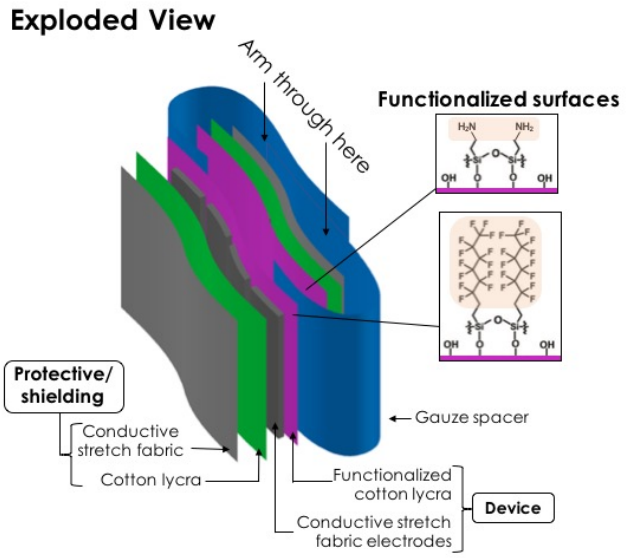

Figure 4: Physical Structure of the Tribexor joint sensor

the noise in the two contacts can be quite different and cannot be completely removed by subtracting the signals.

Solution - part 1: The conductive shield The first stage of our solution uses a textile-based shield to isolate the inner and outer electrodes from noise sources. This is possible by adding additional conductive layers above and below the electrodes to act as a Faraday cage for our textile layers. Our design is shown in Figure 4. The electrodes and functionalized fabric are covered with one layer of plain cotton lycra, used as a dialectric, and one layer of conductive silver nylon fabric that together act as a Faraday cage to shield the triboelectric device from the effects of electric fields. The blue layer is a two-ply gauze fabric used to enhance separation of the triboelectric layers and as a structural element that allows Tribexor to be integrated with a shirt or used as a stand alone sensing sleeve.

Solution - part 2: Differential amplifier The second stage of our pipeline is a differential amplifier. The most important use of the

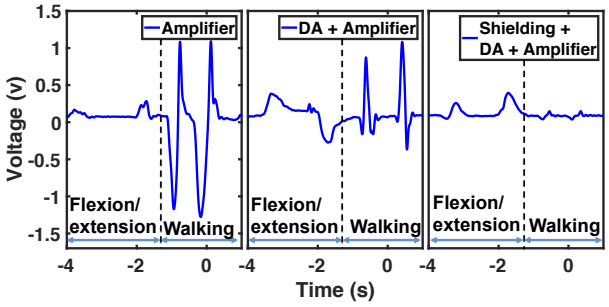

Figure 5: Here we show a breakdown of each noise filtering stage: (left) Amplifier increases signal but the triboelectric signal is barely visible whereas the undesirable static field noise during walking is very large, (middle) Differential Amplifier (DA) increases the signal and reduces noise, (right) Textile shielding removes most of the static field signal and retails the triboelectric signal.

differential amplifier is to enhance the signal since during charge transfer, one of the charge carrying layers becomes more positively charged, and the other more negatively charged. Additionally, it also helps to attenuate some of the static field and 60 Hz powerline noise, although not all of it since the conductive charge gathering contacts are not capturing identical noise profiles as previously mentioned.

Solution - part 3: Analog filtering and amplification stages Since there is still significant residual noise after the differential amplifier, we need additional filtering stages to reduce the noise level. To calculate gain and filtering order of our analog circuit, our goal is to reach an SNR 0f 10 dB and a final triboelectric signal amplitude of 1 V to fully utilize the dynamic range of the ADC used in the wearable system. We set the cut-off frequency of the filtering stages to be 10 Hz to fully capture the fastest anticipated human movements. The overall gain of the circuit can be calculated as:

$$Gain_{dB} = 10log(\frac{V_{out}}{V_{in}})^2 \Rightarrow Gain_{dB} = 60dB \quad (1)$$

And the order of the filtering stage is calculated in Eqn 2.

$$log(\frac{F_{rej}}{F_c}) \times \alpha \times N > 10 - (P_{signal} - P_{noise}) \quad (2)$$

Note that α is the slope of the first order filter, which is 20 dB/decade and N is the target order of designed filter. F_{rej} is the frequency to be rejected, in this case 60 Hz, and F_c is the 3 dB cut-off frequency of our filter. P_{signal} and P_{noise} are the power of the signal and noise at the output node of the differential amplifier, respectively. Consequently, a 4th order filtering is required. Taking these parameters into consideration, we designed the amplifier stages as shown in Figure 3.

Demonstrating the combined effect: How well does our solution work? Figure 5 breaks down the effect of each of the stages of our solution. We omit the initial raw signal since this visually looks like a flat line where the signal is undetectable. If we amplify this signal using our four-stage amplifier, the signal corresponding to joint movement can be seen as relatively small changes but the noise

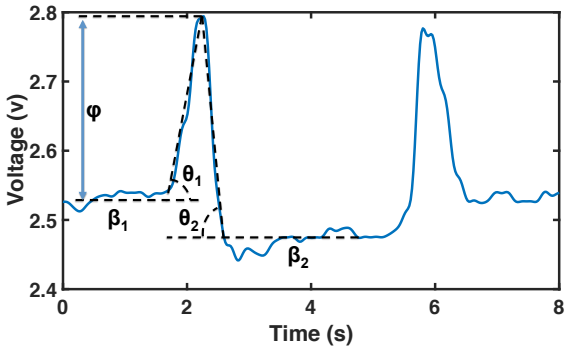

Figure 6: Tribexor's output in response to a flexion followed by an extension. Features used in inferring joint state are annotated.

from walking is substantial and dominates. If we add the differential amplifier, the joint movement signal becomes a lot stronger for reasons explained earlier. This stage also removes some of the 60 Hz and static field noise but not all of it. Finally, if we include the textile shielding, it removes most of the noise while retaining most of the triboelectric signal.

4 INFERRING JOINT STATE AND SWEAT CONCENTRATION

We now turn to analyzing the characteristics of the de-noised signal from Tribexor. We obtain two signals of interest from our sensor. The first is the fast varying changes during flexion and extension of the joint (the phasic component). The second is the slow varying changes due to the state of the joint (the tonic component), which is the change in baseline that can be observed while the joint is stationary. These two signals can be separated from one another by utilizing a low-pass filter. The reason these are both of interest is that the phasic component is useful for identifying specific joint movements, whereas the tonic component provides information about the wetness and salt content in the textile, thereby allowing it to be used to sense exposure to sweat. We describe these two signals in more detail in the coming sections.

4.1 Inferring Joint State

We first look at the dynamic or phasic component of the time-series voltage signal from the textile sensor, and ask how we can map from voltage to the direction of joint movement and the velocity of joint movement. To understand this, we need to obtain an in-depth understanding of the signal characteristics.

Understanding signal characteristics: Figure 6 shows an output instance of an elbow flexion and extension. There are three key parameters of interest: a) the charge and discharge rates annotated as θ_1 and θ_2, b) the baseline voltage when the joint is in the extended vs flexed static position annotated as β_1 and β_2, and c) the peak height of the flexion/extension, ϕ. We now explain how these parameters can be used to determine joint state.

The *charge and discharge rates* (θ_i) of the textile vary according to the start and end state of the textile. At the start of an extension motion, the textile is in a compressed state. As the arm is extended, the layers separate, causing a voltage peak at roughly the midpoint of motion; the voltage subsequently decays because of conductive paths between the textile layers. During a flexion action, the same signal features occur, but at different relative rates. Initially, there is much less surface contact between the textile layers; during motion, a peak still occurs because of separation but at a slower rate. The final state of the textile is a compressed state which results in fast voltage discharge because of more conductive paths available between the textile layers. As a result of this behavior, we consistently find that $\theta_1 > \theta_2$ during extension, and $\theta_1 < \theta_2$ during flexion.

The *signal baseline* (β_i) also changes depending on whether the joint is in the flexed vs extended static position. There are two reasons behind the change. First, the effective surface area and intimacy of contact with the skin will vary as a joint opens or closes. We expect that more EM noise is injected when capacitive coupling is higher, while less is injected when coupling is lower. Second, the impedance between the electrodes and ground plane shielding cause asymmetric signal changes at the input of the differential amplifier. The inputs of the amplifier are the base nodes of BJT transistors. As the impedance of electrodes changes, the bias current of the differential amplifier changes which results in a very small voltage shift in the output of the differential amplifier. This offset, though small, is amplified and is observed as a baseline shift i.e. $\beta_1 > \beta_2$.

The *peak height* (ϕ) depends on the velocity of the joint since the tribo layers move more quickly relative to each other, relating in more compression and expansion and therefore greater amount of charge transfer.

Determining joint state: Given this behavior, it is easy to see how these three parameters can be leveraged to determine joint state and velocity. To distinguish direction of joint motion i.e. whether the joint flexed or extended, the charge/discharge rates (θ_i) and the signal baseline (β_i) are the most useful. To determine velocity of joint motion, the peak height (ϕ) during flexion/extension is most useful.

From a detection standpoint, these observations give us *explainable* features that can be used to distinguish between joint states. Such explainability is increasingly important, particularly when designing robust classification methods.

4.2 Continuous Sweat Monitoring

So far, we have looked at the dynamic or phasic components of the triboelectric signal. We now turn to the slowly varying baseline signal or the tonic component. While sweat monitoring was not our original purpose, our experiments revealed that the baseline signal varied due to sweat which can be used as an additional sensor signal.

Why does sweat affect the output signal? The reason is because the wetting happens in one direction — the inner layers absorb more sweat whereas the outer layers that are close to air are more dry. This results in an impedance difference between the outer and inner electrodes. As depicted in Figure 3, R_1 and R_2 represent the impedances between the outer electrode and shielding layer and inner electrode and shielding layer, respectively. Since sweating initially affects internal layers, it reduces R_2. As a result, a small DC

offset is generated at the output node of the differential amplifier. This small voltage is then amplified in the electronics circuits to create an observable change at the output of Tribexor.

The sweat-induced changes can either be viewed as a useful signal to measure sweating behavior or as noise that confounds the joint measurement signal. If viewed as noise, we can coat the insulation layer between shielding layer and charge collecting electrodes with a hydrophobic coating so as to make it water-repellent [37]. In this work, we look at sweat as a useful biochemical signal that can be captured by Tribexor in addition to its use as a joint movement sensor.

5 IMPLEMENTATION

Our current implementation of Tribexor was the result of several design iterations that evolved as we evaluated the signal output of triboelectric textiles in real-world settings. The first version of Tribexor consisted of a woven arrangement of positive and negative charge carrying threads and collection electrodes. We found that the total surface area of interaction between tribo materials was insufficient to produce a significant signal output. The second version of Tribexor saw the transition to the layered design we described in §3. The increased surface area in the layered design allowed us to see significant signal magnitude changes that correlated with joint motion when worn, but we discovered that this DC signal change was actually coupled electromagnetic noise that changed depending on the amount of coupling with the arm that was related to position and not velocity. This observation motivated us to include the differential amplification stage, which caused signal peaks from triboelectric charge and discharge to become visible at the beginning and end portions of individual arm motions. The addition of a microcontroller and BLE radio allowed us to perform untethered experiments with mobile users; however, we observed charge/discharge peaks that correlated with foot impact while walking. This observation resulted in the final prototype that includes signal shielding layers on either side of Tribexor to reduce static field coupling from outside the measured joint. We now describe this final design in greater detail (depicted in Figure 10).

Layered Textile Sensor The layered textile is comprised of multiple sheets of cotton/lycra spandex (90%/10%, Dharma Trading Co.) and silver-plated nylon/elastic fiber (76%/24%, LessEMF.com) fabrics. To chemically alter the cotton lycra surfaces for tribo functionality: purchased fabric was cut and washed by sonicating in deionized water for 15 minutes to remove any stray fibers or particles from the surface. The swatches were then rinsed with isopropanol and air-dried before soaking for 25 minutes in their respective solutions, which included 1% by vol. trichloro(1H,1H,2H,2H-perfluorooctyl)silane in hexanes for the negatively-charging surface and 10% by vol. (3-aminopropyl)trimethoxysilane in isopropanol for the positively-charging surface. After, the swatches were rinsed with their respective solvents, hexanes or isopropanol, in order to remove excess, unreacted solutes, then air-dried before constructing the Tribexor.

To assemble Tribexor, the stretchy silver nylon fabric was cut into six 6 in. x 1.5 in. strips and sewn around the strip perimeters onto the active tribo layers (three strips to a functional layer, making three devices in total.) Another layer of pristine (unfunctionalized, as received) cotton lycra was then attached by sewing around the perimeters of the strips, leaving one short side unsewn for access to electrical wire connections. Finally, a second layer of 8 in. x 8 in. pristine cotton lycra with a layer of 7 in. x 7 in. silver nylon stretch fabric centered on the back side was attached around its edges on top of the first pristine cotton lycra layer. Altogether, Tribexor layers from the outside in are as follows: silver nylon, 2 cotton lycras, silver nylon electrode strips, tribo-active layer 1, gauze spacer, tribo-active layer 2, silver nylon electrode strips, 2 cotton lycras, silver nylon. The gauze spacer layer covers one inch inward from the edges on opposite sides of the Tribexor, extending outward on both sides to wrap around the limb of the person testing the device. Velcro strips on the gauze allow the user to adjust the size of Tribexor.

The two outermost shield layers (pristine cotton lycra with silver nylon back) are connected with braided wires and are adhered to the fabric using conductive adhesive. The two charge collection layers of a single device are connected to the inputs of the differential amplifier with a similar wire and are also adhered using conductive glue.

Electronics and Software The signal processing, computation, and communication elements of Tribexor are provided by a 4 layer 3.2 cm x 2.3 cm printed circuit board that we designed and a Blufruit Micro MCU with a BLE radio. Our PCB board uses an AD629 differential amplifier with unity gain and a gain stage that consists of 4 BA10324A operational amplifiers; the overall gain and cutoff frequency of the amplification and filtering stages is 60 dB and 10 Hz. The output of the gain stages is fed to the attached Arduino. We collect a stream of ADC values at 80 Hz for further analysis. The electronics circuit board draws roughly 2 mA of current from a 3.3 v power supply. We note that our focus was on signal analysis of an all-textile joint sensing device rather than power consumption and form-factor, and there is significant room for optimization on both fronts.

The motion capture room used for collecting ground truth data is equipped with a Qualisys Oqus Infrared Motion Capture System.

Digital filtering is performed on the voltage signals to reject high frequency noise. For motion detection, a band-pass filter is used to detect the triboelectric signal regardless of the DC level. Finally, for sweat detection, a low-pass filter is applied to the output signal to track the voltage baseline.

6 EVALUATION

Our evaluation shows the advantages of Tribexor for joint and perspiration sensing through a combination of benchmarks and natural experiments.

6.1 Joint Sensing Performance

Tribexor can sense many markers pertaining to joint movement. In this section, we present a few careful benchmarks with a single user and then present a more complex case study with more users.

Flexion vs Extension Detection: Our first set of benchmarks looks at how well we can separate flexion versus extension of the joint using the features shown in Figure 6. We only look at the utility of the two core features θ_i and β_i to understand how useful these two features are to performance.

		Flexion		Extension		Accuracy
		Precision	Recall	Precision	Recall	
Elbow	Stationary (Dry)	.986	.964	.989	.968	.976
	Stationary (Wet)	1.00	1.00	1.00	1.00	1.00
	Walking (Dry)	.881	.881	.881	.881	.881
Knee	Stationary (Dry)	.924	.895	.894	.923	.903

Table 2: Precision and Recall of Flexion and Extension Classification under different conditions

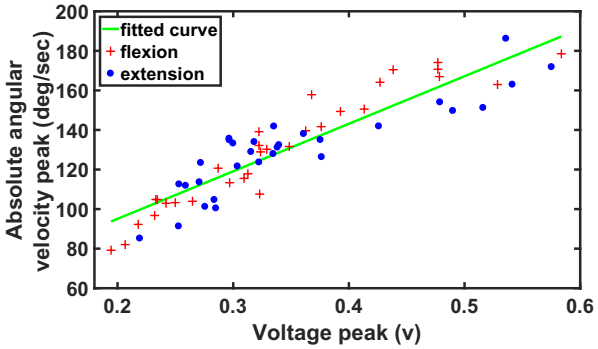

Figure 7: We record different arm velocity motions along with ground truth and find that a linear function describes the relation between signal peak voltage and angular velocity.

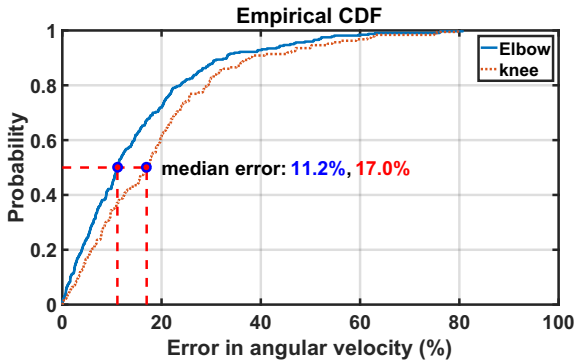

Figure 8: CDF plot for error in angular velocity estimation across multiple wears of the textile. The median error is 11% for the elbow and 17% for the knee.

Let us first look at results for the elbow joint. We collect motion data by having a user perform flexion and extension arm motions for 5 minutes. We then use this data to train a logistic regression based classifier. The classifier is then tested on the same user for data during several different experimental conditions including wearing a moist sleeve, walking while performing the action, and wearing the sleeve in different positions.

Results for binary classifications are summarized in Table 2; we are able to detect flexion and extension with very high precision and recall across a range of conditions. Our best results are measured during benchmark experiments when moisture was introduced – we observed that Tribexor achieves perfect precision and recall as a consequence of larger shifts in DC baseline magnitude. Our worst results were obtained from benchmarks collected while a user was walking, but still yielded precision and recall values of 88.1%; we hypothesize that small shifts in the textile and low amplitude static coupled noise could result in low-velocity joint motions being misclassified.

We perform a similar study for the knee joint. We collected data while a seated user flexes and extends their knee periodically across a range of speeds. A logistic regression classifier is trained for this joint to do the binary classification between knee extension and flexion. The results are quite good for the knee joint as well as shown in the last row of Table 2.

Estimating angular velocity: Next, we look at how well Tribexor can estimate angular velocity of the elbow and knee joint. First, we look at data from the elbow joint from a single user and look at the relationship between the peak height (ϕ in Figure 6) and the joint velocity measured using a motion capture system. Figure 7 validates our intuition and shows that the peak height is indeed linearly related to angular velocity.

Next, we look at how well Tribexor can estimate angular velocity across multiple wears of a textile. While in general, the voltage extracted is highly correlated with the angular speed, loosely worn textiles like sweatshirts are often worn over different inner layers. In addition, the fabric folding and compression may differ slightly each time the textile is worn leading to signal differences.

To characterize the error, we ask the user to remove and re-wear the shirt five times. We then used five-fold cross validation where we calibrated the sensor from data from four of the times the textile was worn, and tested the performance on the held-out data, and repeated this five times.

Figure 8 shows a cumulative distribution of the error. Our results show that, as expected, there is error due to differences across the times when the textile is worn. But we also see that the median angular velocity error is only 11% for the elbow and 17% for the knee. This means that despite the fact that Tribexor is integrated with loose clothing, it provides a reasonable estimate of the velocity under natural settings.

Minimum sensitivity: We now look at the sensitivity of Tribexor i.e. what is the minimum joint velocity that can be detected using the captured signal. According to [19], the typical peak angular velocity for an elbow joint during curl exercises is approximately 200 deg/sec. So, our objective is to be able to detect a signal well below this peak speed so that we can capture the entire flexion and extension motion.

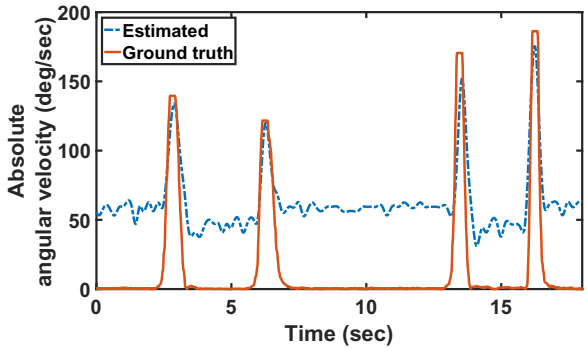

Figure 9: Comparison between reconstructed angular velocity and ground truth for elbow flexion and extension.

Figure 10: User wearing Tribexor implemented as a sleeve.

Figure 9 compares the estimated angular velocity against ground truth when a user is flexing and extending their arm at moderate speeds. We see that the minimum sensitivity is roughly 50 $degrees/second$. The primary reason for this minimum threshold is that we used fixed gain parameters rather than an Automatic Gain Control (AGC) circuit. We expect that future hardware revisions should be able to improve sensitivity. Once we cross the minimum sensitivity, Tribexor tracks the ground truth signal very accurately. Thus, these benchmarks show that Tribexor is a reliable joint sensor and is sufficiently sensitive to capture normal hand movements.

Case Study: Activity recognition — We now turn to a less controlled user study to examine how Tribexor performs in a natural setting. Our case study examines the benefits of Tribexor for recognizing a variety of activities that involve the elbow including eating, walking, and brushing. There has been a significant amount of work on recognizing these activities using inertial sensors on wristworn devices [8, 23]. Our goal is to show that Tribexor can provide an equivalent capability with just loosely worn textiles.

In this experiment. 14 participants (9 male, 5 female) were asked to wear the shirt with Tribexor sewn on. The users wore a medium

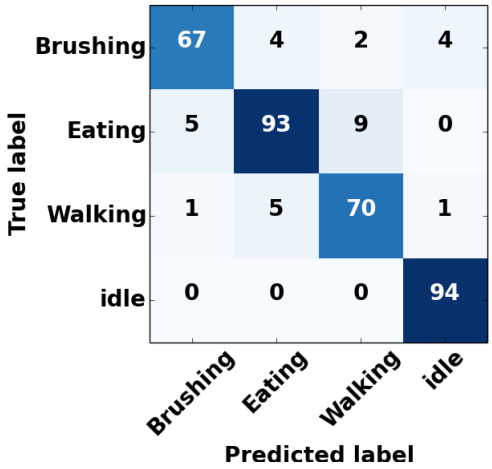

Figure 11: Signal features computed from Tribexor can be used to distinguish between 4 different activity classes with high accuracy.

sized shirt on which Tribexor was sewed to the elbow, as shown in Figure 10. Participants were asked to perform the following activities as normal: eating chips and drinking water, brushing their teeth, walking, and staying still. They were not restricted to a limited eating/drinking pattern. As a result, participants followed their own unique way of eating/drinking (holding a drink or bag of chips in one hand or leaving them on the table, reaching for water or chips at will and placing them wherever they wanted after use). The measurements were performed in an office environment with non-participants walking around in the vicinity during measurements. Participants were aged from 24 to 35 years old. Their height ranged from 5'3" to 6 ft, they weighed from 117 to 220 lbs. We also measured the elbow circumference for each user to ensure that our results were not sensitive to looseness of wear. In our experiment, the elbow circumference of participants ranged from 9 to 12 inches. In total, we collected 110 minutes of data which were almost equally distributed among mentioned activities and users. Ground truth was obtained by recording video and hand-labeling the activity instances by checking timestamps recorded by Tribexor.

We segmented the data into windows and extracted several features from the data as summarized in Table 3. We use several features in addition to the core features since activities span longer timescales and have more variability. We used a standard SVM classifier and five-fold cross validation to classify between the different activities. Our results showed that the SVM classifier can successfully classify the test activities with 91.3% accuracy. Figure 11 shows the confusion matrix for this classification.

6.2 Sweat Sensing Performance

Next, we turn to the sweat sensing capability of the triboelectric textile. To undertand this, we empirically explored the correlation between the reading obtained from Tribexor with a variety of other measures — salt concentration, water volume, and skin conductance from a Galvanic Skin Response (GSR) sensor. The results we show

Feature	Description
Statistical features	We use several statistical features including the signal average, quartiles, standard deviation, and cross-correlation across windows. These provide information about elbow angle changes and variations over different time-spans.
Frequency domain features	Human elbow movements are often distinct in the frequency domain, particularly for hand-to-mouth actions like eating, drinking, or smoking, and periodic movements during brushing and sports activities. We look at the top frequency peaks, as well as the signal power.
Magnitude features	We look at the signal envelope and peaks including peak density and peak height. Peaks capture information about the fast elbow movements.

Table 3: Features used for activity classification. In addition to core features, we extract several other features relevant to activity detection.

are based on a rather laborious process since once we wetted the sensor in a particular way, we need to machine dry it before we use it again.

Estimating sweat level from the triboelectric signal: We now look at how well Tribexor can detect the concentration of sweat. To understand this, we design a controlled measurement setup where we spray the textile with salt water with 40 mMoles of salt concentration, which is similar to that of human sweat. The textile is wrapped around a cylinder shaped object to act as human elbow. During the measurement, the textile is placed on top of a precise digital balance that is used to manually record the textile weight as an indication of salt water applied to the textile.

To better simulate human sweat, we manually adjust rate of water deposition to match normal rate of human sweating. According to [16], the average human sweats at rate of 13 $ml/minute$. The arm accounts for roughly 10% of body surface [30], so we assume that roughly 1.3 $ml/minute$ is generated by the joint. Salt water is applied on front half of the textile which covers around $1/6$ of human arm. As a result, solution is sprayed on the textile at rate of 0.2 $ml/minute$ to best mimic human sweating.

Since we only care about the changes in the baseline signal i.e. β in Figure 6, we use a low-pass filter to remove triboelectric signals generated from hand movements. The result is only the baseline changes due to salt-water accumulation.

Figure 12 shows the changes in baseline, β, as a function of salt water volume. The voltage baseline has a clear second order polynomial relation to salt water volume with a low RMS error of 0.1 V. While there will be natural variations in sweat accumulations in the textile due to evaporation, our results are promising since it provides a fabric-based method to measure sweat.

Case Study 1: Measuring Perspiration During Exercise — We now look at the ability to detect the sweat concentration on a user's skin during strenuous activities. This provides an additional metric of exertion for the user in addition to running speed or heart rate. To demonstrate this, we asked a user to wear Tribexor on their elbow while wearing an Affectiva Q sensor on their wrist [24]. The Q sensor provides an indirect measure of skin moisture level by using skin conductivity as a proxy. We use this as a gold standard metric to evaluate the effectiveness of Tribexor. To detect sweating, we apply a low pass filter on the signal output to reject high-frequency noise. The resulting output represents a baseline for different elbow states. The user was asked to perform a combination of walking and running on a treadmill. There were no restrictions on running or walking speed, arm position or swing, or rest periods where the user

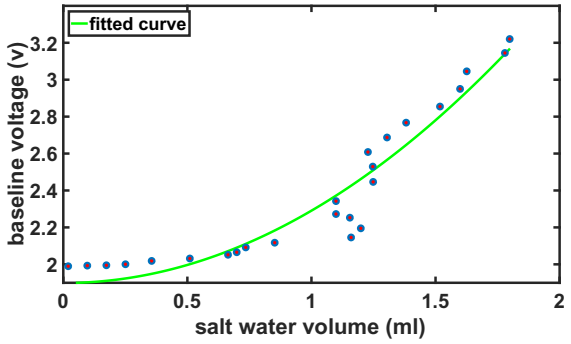

Figure 12: We measure Tribexor's baseline signal output as a function of controlled increases in salt water volume and find a 2nd order polynomial relationship.

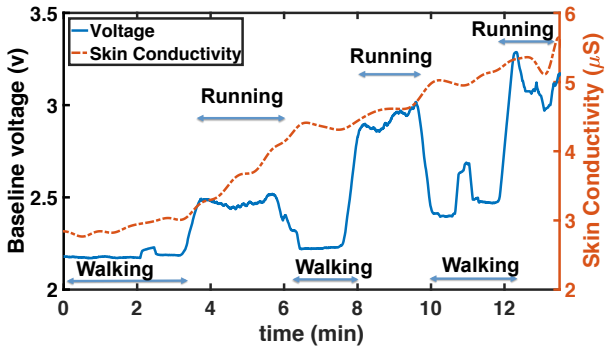

Figure 13: The baseline signal output can be used to measure sweat levels during exercise. We show that Tribexor's signal output roughly tracks skin conductivity, which is used as a measure of skin moisture level.

consumed water. Tribexor's output was collected at a sampling rate of 50 Hz, while the Q sensor was configured to use its maximum sampling rate of 8 Hz. The two sensor streams used a common clock to synchronize prior to the start of the experiment.

Figure 13 shows the extracted signal baseline together with the measured skin conductivity. The results are interesting and show that the signal provided by Tribexor closely tracks the signal from

a GSR sensor but simultaneously provides more information about the current activity state.

Let us first look at the correlation with the GSR sensor. A GSR sensor monitors skin conductivity between two electrodes to measure stimulus that makes sweat glands become more active and allows current to flow more readily. The Tribexor signal is also a cumulative effect of sweat on the resistance of the textile, hence this tracks the GSR reading. This result provides evidence that Tribexor can provide an equivalent signal as GSR. GSR sensors are widely used as a signal of psychological or physiological arousal. The fact that Tribexor provides a similar signal demonstrate a novel textile-based version of a galvanic skin response signal that requires no electrodes.

The second observation is that the phasic (dynamic) component of the signal also shifts when the user is walking vs running. This is because the elbow state is different in walking and running. Users run with their elbows bent which increases the compression between the grounded shielding layers and charge collection layers. This results in a shift in the baseline resulting in a higher voltage level. When the user starts walking, their elbow extends more and results in a reduced baseline. Thus, we see that by analyzing the phasic and tonic components of the signal we can obtain complementary information about the joint.

Case Study 2: Comfort Level Detection for Smart HVAC Systems — Our final case study further explores the sweat sensing capability of Tribexor. In this application, we focus on determining users' comfort levels in controlled climate environments such as homes, offices, or cars. For example, one possible scenario is HVAC monitoring during nighttime where the textile monitors sweating and adjusts temperature.

In this study, we demonstrate Tribexor's ability to detect the comfort of a car passenger. To do this, we set the car's temperature to 90°F, which is outside of a typical human's comfort zone. We then monitor the voltage output of Tribexor as well as the Q Sensor as in the previous case study to provide a gold standard measure of sweating behavior. We simultaneously record the car's temperature using a portable temperature and humidity sensor. In contrast to the previous case study, the user remains mostly stationary in a position that roughly corresponds to that normally used while driving – the user's right hand (same arm instrumented with Tribexor), is occasionally moved between the steering wheel and shifter. We remove the dynamic changes due to hand movements and focus on the changes in baseline.

Figure 14 shows Tribexor's output altogether with skin conductance and temperature. The figure shows that as the measured baseline signal output begins to increase quickly when the temperature value moves above ~73 degrees F, which is roughly the temperature that exceeds the comfort zone of a typical human. When the car's temperature increases above 80 degrees F, we see a sharp increase in Tribexor's output, as well as the Q sensor, indicating that the user may be well outside of their personal comfort zone. This metric is especially useful because it takes into account other information that varies across users and context, such as their body type or number of layers of clothing they are wearing. All of these can change the ideal comfort temperature for a particular user, and Tribexor allows us to measure these changes.

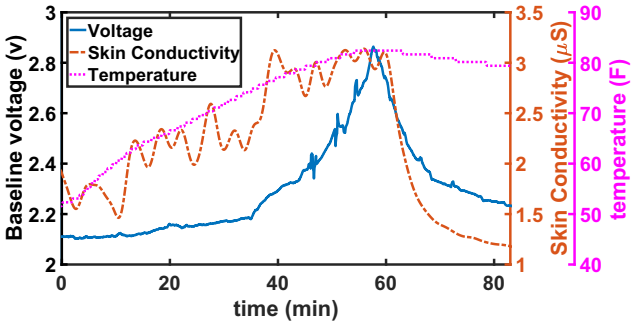

Figure 14: Tribexor can also be used to measure elevated skin moisture caused by thermal discomfort. Here we show the baseline signal output significantly increases when a user is taken outside of their thermal comfort zone; we validate this result with wrist skin conductivity.

7 DISCUSSION

We now discuss some of the limitations of our current approach and avenues of future work.

Tribexor is a fabric-based device and while we were able to deal with moderate wetness, the output was too unpredictable at high levels of wetness. Since we were also interested in measuring skin moisture level, we chose not to use water repellent fabrics in our current design but this could be an option if the device needs to operate at higher wetness levels.

While we have demonstrated the basic functionality of Tribexor, there are many exciting directions that are enabled by this new sensing technique. One direction is instrumenting clothing with multiple instances of Tribexor to sense multiple joints simultaneously. For example, smart textile patches in an elderly individuals' pant legs can monitor gait to detect imbalance that might indicate neurological disease progression. Since Tribexor can be placed at multiple joints where clothing is worn, it can be used to monitor user's movements during long periods of time with less burden on the user. This would be particularly useful for elder monitoring and degenerative illness progression tracking, such as Osteoartheritis and Parkinson's disease. Similarly, Tribexor could be used to track a user's rehabilitation progress after recovering from injury or surgery. Another direction is combining energy harvesting with triboelectric sensing. Triboelectric textiles generate a small amount of energy during movement which can potentially be leveraged to improve the energy-efficiency of smart textiles.

8 CONCLUSION

In this work, we presented the design of Tribexor, an end-to-end sensing system that leverages triboelectric textiles to measure joint motions and sweating behavior. While triboelectric textiles have been evaluated in lab environments, our work takes this technology from the lab to the natural environment and addresses challenges in reducing noise, understanding signal characteristics and extracting useful features. We quantified the performance of Tribexor by benchmarking its robustness as well as through real-world performance

evaluation across three application case studies including activity classification, perspiration measurements during exercise, and comfort level detection for HVAC systems. In our future work, we aim to extend joint sensing to the entire body and focus on clinical metrics including gait differential and athletic performance applications that focus more on joint motion accuracy. We also plan to better optimize the device itself by exploring fabrication techniques that combine the individual textile layers and leverage harvested triboelectric energy to power other system components.

Acknowledgements

We thank our anonymous shepherd and the reviewers for their helpful feedback on the paper. This research was partially funded by NSF award #1763524.

REFERENCES

[1] Athos. https://www.liveathos.com/. (Accessed on 04/05/2018).
[2] Jacquard by google | home. https://atap.google.com/jacquard/. (Accessed on 04/05/2018).
[3] Jacquard by google | levi's collaboration. https://atap.google.com/jacquard/levi/. (Accessed on 04/05/2018).
[4] Nike men's aeroreact. nike.com. https://www.nike.com/us/en_us/c/running/mens-aeroreact. (Accessed on 04/05/2018).
[5] The polotech game plan. http://www.rlmag.com/us/en/magazine/the-polo-tech-fitness-plan. (Accessed on 04/05/2018).
[6] Technology | under armour | us. https://www.underarmour.com/en-us/technology. (Accessed on 04/05/2018).
[7] L. Allison, S. Hoxie, and T. L. Andrew. Towards seamlessly-integrated textile electronics: methods to coat fabrics and fibers with conducting polymers for electronic applications. *Chemical Communications*, 53(53):7182–7193, 2017.
[8] F. Attal, S. Mohammed, M. Dedabrishvili, F. Chamroukhi, L. Oukhellou, and Y. Amirat. Physical human activity recognition using wearable sensors. *Sensors*, 15(12):31314–31338, 2015.
[9] L. B. Baker. Sweating rate and sweat sodium concentration in athletes: a review of methodology and intra/interindividual variability. *Sports Medicine*, 47(1):111–128, 2017.
[10] S. Coyle, D. Morris, K.-T. Lau, D. Diamond, N. Taccini, D. Costanzo, P. Salvo, F. Di Francesco, M. G. Trivella, J.-A. Porchet, et al. Textile sensors to measure sweat ph and sweat-rate during exercise. In *Pervasive Computing Technologies for Healthcare, 2009. PervasiveHealth 2009. 3rd International Conference on*, pages 1–6. IEEE, 2009.
[11] C. Dalsgaard and R. Sterrett. White paper on smart textile garments and devices: a market overview of smart textile wearable technologies. *Market Opportunities for Smart Textiles, Ohmatex, Denmark*, 2014.
[12] K. Dong, J. Deng, Y. Zi, Y.-C. Wang, C. Xu, H. Zou, W. Ding, Y. Dai, B. Gu, B. Sun, et al. 3d orthogonal woven triboelectric nanogenerator for effective biomechanical energy harvesting and as self-powered active motion sensors. *Advanced Materials*, 29(38), 2017.
[13] P. T. Gibbs and H. Asada. Wearable conductive fiber sensors for multi-axis human joint angle measurements. *Journal of NeuroEngineering and Rehabilitation*, 2005.
[14] G. Gioberto, J. Coughlin, K. Bibeau, and L. E. Dunne. Detecting bends and fabric folds using stitched sensors. In *Proceedings of the 2013 International Symposium on Wearable Computers*, pages 53–56. ACM, 2013.
[15] X. He, Y. Zi, H. Guo, H. Zheng, Y. Xi, C. Wu, J. Wang, W. Zhang, C. Lu, and Z. L. Wang. A highly stretchable fiber-based triboelectric nanogenerator for self-powered wearable electronics. *Advanced Functional Materials*, 27(4):1604378–n/a, 2017. 1604378.
[16] C. Jessen. *Temperature regulation in humans and other mammals*. Springer Science & Business Media, 2012.
[17] Q. Jing, G. Zhu, W. Wu, P. Bai, Y. Xie, R. P. Han, and Z. L. Wang. Self-powered triboelectric velocity sensor for dual-mode sensing of rectified linear and rotary motions. *Nano Energy*, 10:305–312, 2014.
[18] K. N. Kim, J. Chun, J. W. Kim, K. Y. Lee, J.-U. Park, S.-W. Kim, Z. L. Wang, and J. M. Baik. Highly stretchable 2d fabrics for wearable triboelectric nanogenerator under harsh environments. *ACS Nano*, 9(6):6394–6400, 2015. PMID: 26051679.
[19] D. V. Knudson. *Fundamentals of Biomechanics*. Kluwer Academic, 2003.
[20] D. T. Lykken and P. H. Venables. Direct measurement of skin conductance: A proposal for standardization. *Psychophysiology*, 8(5):656–672, 1971.
[21] C. Mattmann, F. Clemens, and G. Tröster. Sensor for measuring strain in textile. *Sensors*, 8(6):3719–3732, 2008.
[22] L. S. Mccarty and G. M. Whitesides. Electrostatic charging due to separation of ions at interfaces: contact electrification of ionic electrets. *Angewandte Chemie*, 47 12:2188–207, 2008.
[23] A. Parate, M.-C. Chiu, C. Chadowitz, D. Ganesan, and E. Kalogerakis. Risq: Recognizing smoking gestures with inertial sensors on a wristband. In *Proceedings of the 12th annual international conference on Mobile systems, applications, and services*, pages 149–161. ACM, 2014.
[24] R. W. Picard. Measuring affect in the wild. In *International Conference on Affective Computing and Intelligent Interaction*, pages 3–3. Springer, 2011.
[25] T. H. M. L. D.-H. K. S. Jung, J. Lee. *Advanced Materials*. 2014.
[26] Y. O. J. L. G. B. Y. L. J. S. S. C. J. K. J. P. J. H. S. Lee, W. Ko. *Nano Energy*. 2015.
[27] S. Shen, H. Wang, and R. Roy Choudhury. I am a smartwatch and i can track my user's arm. In *Proceedings of the 14th annual international conference on Mobile systems, applications, and services*, pages 85–96. ACM, 2016.
[28] H. J. Sim, C. Choi, S. H. Kim, K. M. Kim, C. J. Lee, Y. T. Kim, X. Lepró, R. H. Baughman, and S. J. Kim. Stretchable triboelectric fiber for self-powered kinematic sensing textile. *Scientific reports*, 6, 2016.
[29] Y. Su, G. Xie, S. Wang, H. Tai, Q. Zhang, H. Du, X. Du, and Y. Jiang. Self-powered humidity sensor based on triboelectric nanogenerator. In *SENSORS, 2017 IEEE*, pages 1–3. IEEE, 2017.
[30] A. Wallace. Burns: some experiences in local care. *British journal of plastic surgery*, 4:224–229, 1951.
[31] X. Wang, Z. L. Wang, and Y. Yang. Hybridized nanogenerator for simultaneously scavenging mechanical and thermal energies by electromagnetic-triboelectric-thermoelectric effects. *Nano Energy*, 26:164 – 171, 2016.
[32] X. Wang, H. Zhang, L. Dong, X. Han, W. Du, J. Zhai, C. Pan, and Z. L. Wang. Self-powered high-resolution and pressure-sensitive triboelectric sensor matrix for real-time tactile mapping. *Advanced Materials*, 28(15):2896–2903.
[33] Z. L. Wang, J. Chen, and L. Lin. Progress in triboelectric nanogenerators as a new energy technology and self-powered sensors. *Energy & Environmental Science*, 8(8):2250–2282, 2015.
[34] K. Young Lee, H.-J. Yoon, T. Jiang, X. Wen, W. Seung, S.-W. Kim, and Z. Lin Wang. Fully packaged self-powered triboelectric pressure sensor using hemispheres-array. 6:n/a–n/a, 04 2016.
[35] L. Zhang, Y. Yu, G. P. Eyer, G. Suo, L. A. Kozik, M. Fairbanks, X. Wang, and T. L. Andrew. All-textile triboelectric generator compatible with traditional textile process. *Advanced Materials Technologies*, 1(9):1600147–n/a, 2016. 1600147.
[36] Y. S. Zhou, G. Zhu, S. Niu, Y. Liu, P. Bai, Q. Jing, and Z. L. Wang. Nanometer resolution self-powered static and dynamic motion sensor based on micro-grated triboelectrification. *Advanced Materials*, 26(11):1719–1724, 2014.
[37] J. Zimmermann, F. A. Reifler, G. Fortunato, L.-C. Gerhardt, and S. Seeger. A simple, one-step approach to durable and robust superhydrophobic textiles. *Advanced Functional Materials*, 18(22):3662–3669, 2008.